Aging Research

ISSN 2957-8701 (print); 2957-9295 (online)
https://doi.org/10.26599/AGR.2024.9340024

Article

A comprehensive prognostic and immune analysis of FDX1 in brain lower grade glioma

Lina Zhang[1,2], Tenghui Ma[2,5,§], Yanling Wang[3,4,§], Jiamin Chen[2] (✉), Wenwen Fu[2] (✉)

[1] *The First Clinical Medical College Guangzhou University of Chinese Medicine, Guangzhou 510080, China*
[2] *Department of Clinical Nutrition and Microbiome; Biomedical Innovation Center, The Sixth Affiliated Hospital, Sun Yat-sen University, Guangzhou 510655, China*
[3] *The Second Clinical Medical College Guangzhou University of Chinese Medicine, Guangzhou 510120, China*
[4] *Department of Rehabilitation Lianyungang Hospital of Traditional Chinese Medicine, Lianyungang 222004, China*
[5] *Department of Colorectal Anal Surgery, The Sixth Affiliated Hospital, Sun Yat-sen University, Guangzhou 510655, China*
[§] *These authors contributed equally to this work.*

Received: 15 March 2024 | **Revised:** 3 June 2024 | **Accepted:** 3 June 2024

ABSTRACT

To investigate the prognostic and immune values of ferredoxin 1 (FDX1) in brain lower grade glioma (LGG). Data from the Cancer Gene Atlas Database and the Genotype and Gene Expression Correlation Database were collected to compare the expression difference of FDX1 between glioma tissues and normal tissues, along with immunohistochemical method. Cox regression analysis was used to evaluate the relationship between FDX1 expression and survival indicators. The Kaplan–Meier method was used to assess independent risk of FDX1 in LGG survival probability. The Tumor Immune Estimation Resource database was used to evaluate the correlation between FDX1 expression and immune cell infiltration. FDX1 was overexpressed in LGG than normal tissues. The Kaplan–Meier analysis showed high FDX1 expression was significantly correlated with poor overall survival, disease specific survival and progress free interval ($P < 0.001$). A positive correlation was found between FDX1 expression and infiltration of B cells, CD4+ T cells, CD8+ T cells, macrophages, neutrophils and dendritic cells. FDX1 was positively correlated with immune checkpoints in LGG. FDX1 may serve as a specific prognostic and therapeutic biomarker for LGG.

KEYWORDS

ferredoxin 1 (FDX1), lower grade glioma (LGG), prognostic biomarker, immune infiltration

1 Introduction

Worldwide, cancer is a serious public health problem, with rising morbidity and mortality. It has become the second cause of death after cardiovascular disease [1]. According to the latest global cancer statistics, the novel cases and cancer-related deaths of central nervous system tumors were 308,102 and 251,329 in 2020, respectively [2]. Glioma is the most common primary intracranial tumor originating from glial cells, representing 80% of all brain malignancies [3]. According to histological features, the World Health Organization (WHO) classified gliomas into brain low-grade gliomas (LGG, I/II) and brain high-grade gliomas (HGG, III/IV) in 2021[4]. LGG accounts for 15% of all glioma, and the 5-year survival rate is 30%–70% [5]. LGG is less malignant than HGG and grows at a lower speed, but it inevitably develops into HGG eventually. At present, gliomas are mainly treated by surgical resection in clinical practice, combined with radiotherapy and chemotherapy [6, 7]. Despite considerable effort has been made to enhance the treatment of LGG, the curative effect and prognosis are not optimistic. Consequently, it's an urgent need to explore potential and useful biomarkers to improve therapy and prognosis for LGG patients.

In recent years, the tumor microenvironment (TME) and immune milieu have earned substantial interest. Tumor immunotherapy aims to kill cancer cells by activating the human immune system [8]. TME is recognized as an essential element of tumor development and progression, and plays an important role in clinical tumor immunotherapy [9]. Cuproptosis is a new type of programmed cell death, which was found and named by Tsvetkov, et al. in 2022 [10]. Copper

✉ Address correspondence to Jiamin Chen, chenjm263@mail.sysu.edu.cn; Wenwen Fu, 15778018802@163.com

Cite this article as Zhang, L. N., et al. *Aging Research*, **2024**, 2: 9340024.

is one of the essential trace elements for all organisms, but it becomes toxic if excessive. Copper binds directly to the lipoylated components of the tricarboxylic acid cycle, leading to toxic protein stress and ultimately cell death. The use of cuproptosis to kill cancer cells may become a new therapy of cancer.

Ferredoxins are a large family of redox proteins. Ferredoxin reductase, the only ferredoxin reductase in humans, transfers electrons from nicotinamide adenine dinucleotide phosphate (NADPH) to multiple cytochrome P450 enzymes through ferredoxin 1 (FDX1) and ferredoxin 2 (FDX2) [11]. FDX1, also known as adrenodoxin or hepatoredoxin, has been reported exerting effect in the metabolism of steroid hormones, bile acids, vitamin A, and vitamin D [12]. The latest research shows that FDX1 is a key regulator of cuproptosis [10]. *FDX1* gene encodes a reductase known to reduce Cu^{2+} to Cu^{1+}, which is more toxic. FDX1 is an upstream regulator of protein lipoylation, and the knockout of FDX1 can save cell cuproptosis. The study of FDX1 is significant for tumor prognosis and treatment in practice.

In this study, we used data from the Cancer Genome Atlas (TCGA) and the Genotype-Tissue Expression (GTEx) to compare the expression of FDX1 in LGG and normal tissues. We investigated the association between the *FDX1* gene expression, clinical features and survival indicators of LGG patients. Meanwhile, we also evaluated the prognostic value of FDX1 in LGG for overall survival (OS) based on TCGA dataset. Furthermore, the link between the FDX1 expression levels and immune cells infiltration was analyzed using data from the Tumor Immune Estimation Resource (TIMER).

2 Results and discussion

2.1 Expression levels of FDX1 in pan-cancer and LGG

We evaluated the mRNA expression of FDX1 in 33 cancer cell lines from the UCSC XENA (https://xenabrowser.net/datapages/). Differential analysis was performed on 33 tumor tissues and the corresponding normal tissues. Based on the Mann–Whitney U test (Wilcoxon rank sum test), 5 of 33 tumor types (bladder urothelial carcinoma (BLCA), cervical and endocervical cancers (CESC), kidney chromophobe (KICH), liver hepatocellular carcinoma (LIHC), and skin cutaneous melanoma (SKCM)) showed no significant difference in expression. 14 tumor types (LGG, colon adenocarcinoma (COAD), lymphoid neoplasm diffuse large B-cell lymphoma (DLBC), esophageal carcinoma (ESCA), glioblastoma multiforme (GBM), lung adenocarcinoma (LUAD), ovarian serous cystadenocarcinoma (OV), pancreatic adenocarcinoma (PAAD), prostate adenocarcinoma (PRAD), rectum adenocarcinoma (READ), stomach adenocarcinoma (STAD), thymoma (THYM), uterine corpus endometrial carcinoma (UCEC), and uterine carcinosarcoma (UCS)) showed higher FDX1 expression than relatively normal tissues, while 11 types (adrenocortical carcinoma (ACC), bladder urothelial carcinoma (BRCA), cholangiocarcinoma (CHOL), head and neck squamous cell carcinoma (HNSC), kidney renal clear cell carcinoma (KIRC), kidney renal papillary cell carcinoma (KIRP), acute myeloid leukemia (LAML), lung squamous cell carcinoma (LUSC), pheochromocytoma and paraganglioma (PCPG), testicular germ cell tumors (TGCT), thyroid carcinoma (THCA)) were lower. As shown in Fig. 1A.

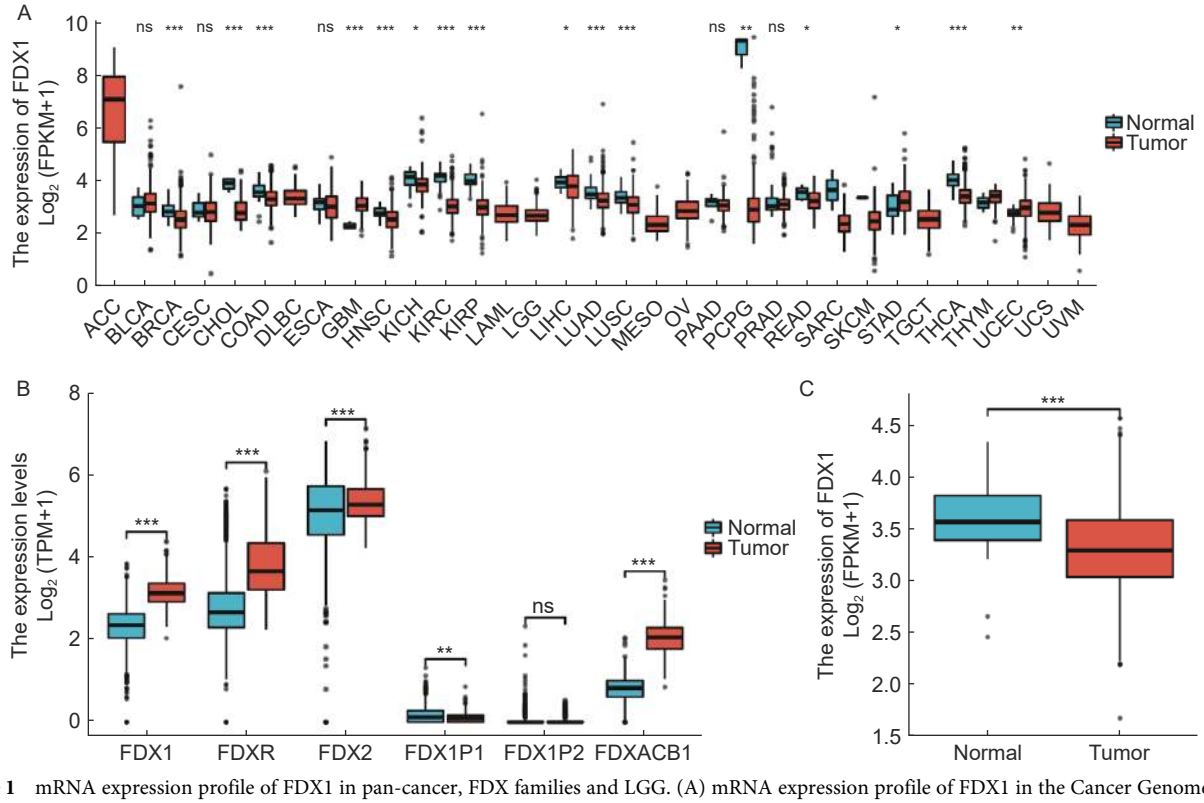

Figure 1 mRNA expression profile of FDX1 in pan-cancer, FDX families and LGG. (A) mRNA expression profile of FDX1 in the Cancer Genome Atlas (TCGA) cohorts. (B) Expression characteristics of FDX family in LGG. (C) Differential expression of FDX1 in LGG and normal tissues. *$P < 0.05$, **$P < 0.01$, ***$P < 0.001$. MESO, mesothelioma; SARC, sarcoma; UVM, uveal melanoma.

We performed the Mann–Whitney U test (Wilcoxon rank sum test) for the expression difference of FDX family in LGG and normal tissues, and the results showed that there was no significant difference in the expression of FDX1P2 ($P > 0.05$). The expression of FDX1, FDXR, FDX2, and FDXACB1 in the tumor group was higher than that in the normal group ($P < 0.001$), and the expression of FDX1P1 in the tumor group was lower than that the normal group ($P = 0.001$). The results were displayed in Fig. 1B.

The expression of FDX1 in LGG and normal tissues was analyzed separately: the median (upper and lower quartiles) of the normal group was 2.359 [2.049, 2.633], and the median (upper and lower quartiles) of the tumor group was 3.136 [2.926, 3.382]. Mann–Whitney U test (Wilcoxon rank sum test) showed that tumor was higher than normal, the median difference between the two groups was 0.808 [0.766, 0.851], the difference was statistically significant ($P < 0.001$), as shown in Fig. 1C.

2.2 Relationship between the expression of FDX1 and clinical features and the prediction of LGG

The result of risk score was shown in Fig. 2A. With increased FDX1 expression, the higher risk score and number of deaths.

The Kaplan–Meier analysis was used to evaluate the association between FDX1 expression with overall survival, disease specific survival and progress free interval in LGG based on the TCGA database. Log-rank test and Cox regression showed that the difference in survival time distribution among group groups was statistically significant ($P < 0.001$). The high group has a worse prognosis than the low group, as shown in Figs. 2D–2F.

Receiver operating characteristic (ROC) curve for 1 year: AUC = 0.621; confidence interval (CI) = 0.523–0.719; cumulative survival rate = 0.944; sensitivity = 0.77; specificity = 0.471. ROC curve for 2 year: AUC = 0.672; CI = 0.602–0.74; cumulative survival rate = 0.856; sensitivity = 0.547; specificity = 0.547. ROC curve for 3 year: AUC = 0.662; CI =

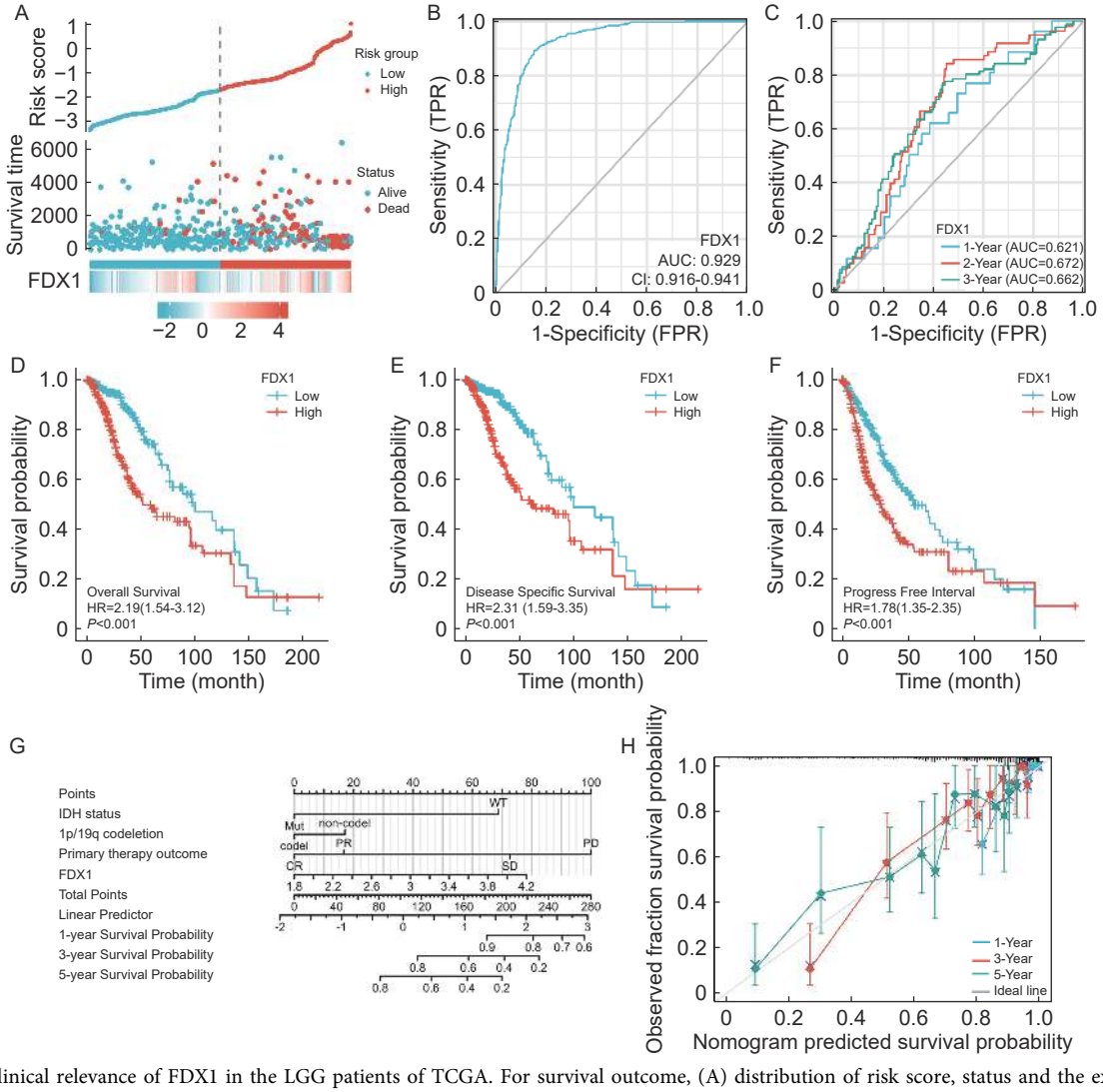

Figure 2 Clinical relevance of FDX1 in the LGG patients of TCGA. For survival outcome, (A) distribution of risk score, status and the expression of FDX1; (B) ROC curves showed the predictive efficiency of the FDX1 for LGG patients based on TCGA cohorts; (C) Based on the TCGA cohort, ROCs for one-year, two-year and three-year OS prediction in LGG patients; (D–F) prognostic for OS, disease specific survival (DSS), and progress free interval (PFI) in LGG patients with FDX1, respectively. True positive rate (TPR) and false positive rate (FPR) are evaluated by Cox proportional hazard models. (G, H) Nomogram development and validation. (G) Nomogram to predict the 1-year, 3-year, and 5-year OS of LGG patients. (H) Calibration curve for the OS nomogram model in LGG. A dashed diagonal line represents the ideal nomogram.

0.587–0.737; cumulative survival rate = 0.771; sensitivity = 0.777; specificity = 0.554. The results were displayed in Figs. 2B and 2C.

2.3 Construction and prediction of prognostic nomogram

In order to investigate the application of FDX1 in cancer prognosis, we built a nomogram for predicting the overall survival of LGG patients in the TCGA cohort. The cancer stage and FDX1 were included as prognostic factors in the nomogram (Fig. 2G). Model Global Statistical Test Status, concordance (*C*)-index = 0.822 [0.802, 0.842], Likelihood ratio test = 103.7 on 6 df., $P \leq$ 2e–16, Wald test = 98.62 on 6 df., $P \leq$ 2e–16, Score (logrank) test = 127.91 on 6 df., $P \leq$ 2e–16.

The calibration curve showed that the nomogram was reliable in predicting possibility of 1-, 3-, 5-years overall survival in LGG (Fig. 2H).

2.4 Analysis of correlation with immune infiltration

A Tumor Immune Estimation Resource (TIMER; cistrome.shinyapps.io/timer) was used to investigate the relationship between the expression of FDX1 and the abundance of six immune cells. The results showed a positive correlation between FDX1 expression and infiltration of B cells, CD4+ T cells, CD8+ T cells, macrophages, neutrophils and dendritic cells (Fig. 3A). We also examined three important immune checkpoints (PD-1, PD-L1, and TIM-3) since the expression level of immune checkpoint-related genes is related to the treatment response of immune checkpoint inhibitors. The Pearson correlation analysis was used to examine the association between PDCD1, PD274, HAVCR2 and FDX1, and all results showed positive correlations. The most significant positive correlation is between FDX1 and HAVCR2, as shown in Figs. 3B–3D.

2.5 Expression of FDX1 protein in LGG and meningioma

The results of immunohistochemical method were showed in Fig. 4. 80% of LGG samples were high expression of FDX1 protein (Figs. 4A–4D), while all the two normal brain tissues of meningioma were negative (Figs. 4F and 4G). This study was approved by the Ethical Committee of the Sixth Affiliated Hospital of Sun Yat-sen University (No. E2023092).

3 Discussion

Gliomas are the most prevalent and intractable malignant tumors of the central nervous system, characterized by unfavorable prognoses, elevated mortality rates, and substantial societal and familial. Gliomas lack specific clinical manifestations. Neatly half of newly diagnosed cases exhibit high malignancy. Despite considerable progress, the majority of patients will inevitably suffer recurrence or drug resistance [13]. Therefore, early diagnosis and effective treatment for LGG are of paramount importance.

As a new mode of regulating cell death, copperoptosis induces toxic protein stress by binding copper to acylated fatty acids in the tricarboxylic acid cycle [10]. The *FDX1* gene plays a pivotal role in regulating copperoptosis. Previous studies have suggested that FDX1 may hold clinical significance in cancer surveillance and treatment. Specifically, low expression of FDX1 is commonly observed in most cancers, whereas high FDX1 expression is associated with improved overall survival and death-specific survival [14]. However, a recent study has demonstrated that FDX1 expression is upregulated in gliomas and is linked to poor prognosis in LGG [15].

To explore the expression of the *FDX1* gene in cancers, TIMER was used to analyze the transcripts level of the *FDX1* gene in 33 types of tumors and normal tissues. We found that the transcriptome expression level of FDX1 were various in different tumors, which was consistent with the previous studies [16]. It suggested that *FDX1* gene seemed to have a complex biological function. Utilizing data from TCGA and GTEx, our analysis revealed a significant upregulation of FDX1 expression in LGG tumor tissues compared to the corresponding normal tissues. This confirmed by the immunohistochemistry we did, although the sample size was limited. Zhang, et al. [17] also used immunohistochemistry to detect the expression of FDX1 in 40 glioma samples and 20

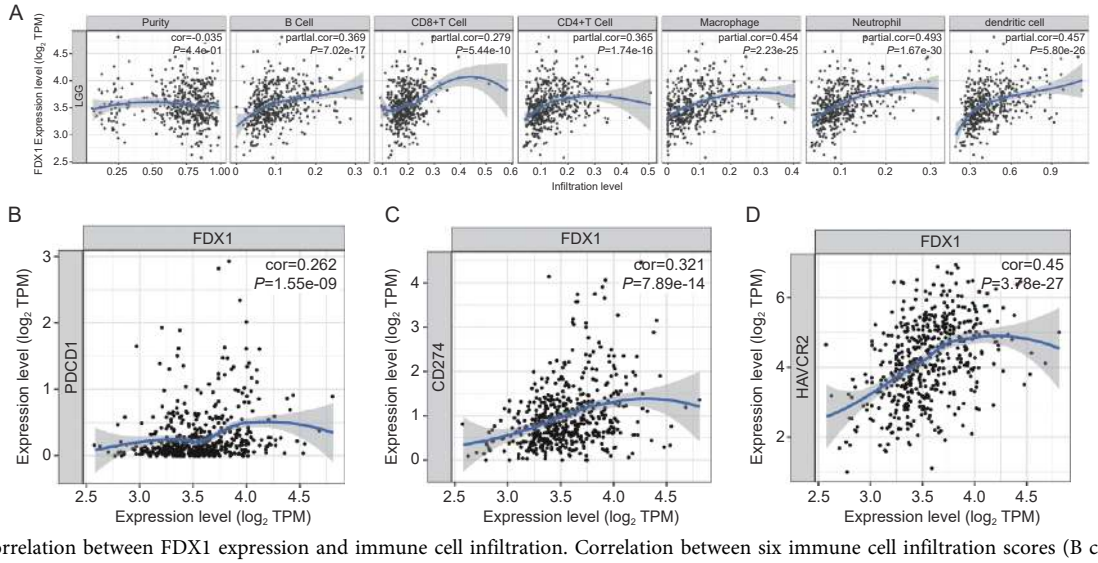

Figure 3 Correlation between FDX1 expression and immune cell infiltration. Correlation between six immune cell infiltration scores (B cell, CD4+ T cell, CD8+ T cell, neutrophil, macrophage, dendritic cell) and FDX1 mRNA expression in LGG. (Spearman correlation test, 0 < cor <1 denotes positive correlation, $P < 0.05$ was considered significant).

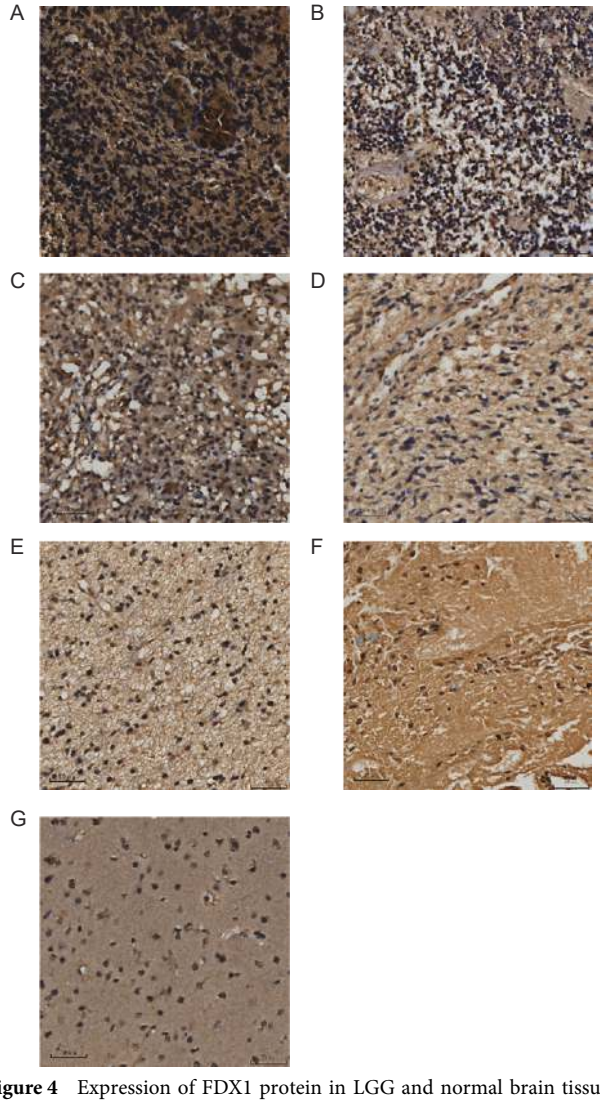

Figure 4 Expression of FDX1 protein in LGG and normal brain tissues (scale bar = 50 μm). (A–D) Positive in LGG. (E) Negative in LGG. (F–G) Negative in normal brain tissues of meningioma.

traumatic brain samples. The immunohistochemical results were scored through a semi-quantitative analysis by pathologists. The expression of FDX1 in glioma samples was significantly higher than that in non-neoplastic brain samples ($P < 0.01$). 57% (8/14) of LGG samples were highly expressed FDX1, but it is regrettable that they didn't compare FDX1 expression levels between the LGG group and the control group.

Zhu, et al. [18] found that FDX1 was an independent prognostic factor and potential prognostic biomarker of glioma. Zhang, et al. [19] found that FDX1 level independently predicted prognosis of WHO grade II/III glioma and might be a valuable therapeutic target. Lu, et al. [15] found that FDX1 expression was associated with overall survival and progression free survival in LGG patients. We carried out the survival prognostic analysis of LGG, and found a positive correlation between FDX1 expression and the risk of death in LGG patients though the TCGA database. Compared with patients with high expression of FDX1, patients with low FDX1 were significantly associated with a better overall survival, disease specific survival and progression free interval rate. It suggested that high expression of FDX1 was an independent predictive factor for poor prognosis of LGG.

The therapeutic effect of tumor immunotherapy mainly depends on the tumor microenvironment. To further figure out the relationship between *FDX1* gene expression and immune cell infiltration in the immune microenvironment of the tumor, we subsequently analyzed the correlation between FDX1 and immune infiltration. The results showed that FDX1 promoted immune infiltration in LGG. Wang, et al. [20] also analyzed the associations between the risk score and infiltration abundances of six types of immune cells in glioma. Except for CD4+ T cells, the infiltration of B cells, CD8+ T cells, dendritic cells, macrophages and neutrophils was positively associated with the prognostic risk score. Lu, et al. [15] analyze the relationship between FDX1 and immune cell infiltration in glioma and found a positive correlation between FDX1 expression and infiltration of CD4+ T cells, T lymphocytes, macrophages, dendritic cells, and negative correlation with B cells. Different immune cells have different effects on tumors [21]. For instance, high B cell infiltration level generally indicate better prognosis, while high macrophage infiltration is primarily associated with a poor prognosis [22–24]. The expression of immune checkpoint genes was one of the key factors affecting the immune microenvironment. In this study, we found significant positive correlation between FDX1 and immune checkpoints in LGG. FDX1 might play a different role in tumors by regulating the tumor microenvironment.

The value of FDX1 in LGG remains unclear. The innovation of this study is that, we found that higher FDX1 expression was strongly correlated with poor prognosis of LGG and enhanced immune infiltration. FDX1 may serve as a novel immunotherapy biomarker in LGG. Our work had several limitations. Most data came from public databases and validated only *in vitro*. We only carried out immunohistochemical method in a few tissues. Prospective studies with larger sample sizes are needed in the future.

4 Conclusion

FDX1 may play an important role in the occurrence and development of LGG. FDX1 level independently predicted prognosis of LGG and regulated the tumor microenvironment. Targeting of FDX1 expression may serve as a specific prognostic and therapeutic biomarker for LGG.

5 Methods

5.1 Data collection and processing

LGG and normal tissue data were extracted from TCGA (https://www.cancer.gov/) and GTEx (https://gtexportal.org/home/datasets), respectively. RNA-seq data in the transcripts per million reads (TPM) format were uniformly processed by University of California Santa Cruz (UCSC) XENA browser (https://xenabrowser.net/datapages) through the Tail process [25]. Expression comparison between samples after $\log_2$ transformation of RNA-seq data in TPM format using R package of "ggplot2" in an R environment (R version: 3.6.3).

The relationship between the expression of FDX1 and the clinical features of LGG

5.2 The relationship between the expression of FDX1 and the clinical features of LGG

RNA-seq data in level 3 HTSeq-FPKM (Fregments Per Kilobase per Million) format is from LGG project in TCGA. Prognostic data were obtained from the journal *Cell* [26]. The FPKM RNA-seq data were $\log_2$ transformed using R package of "survminer" in an R environment (R version: 3.6.3). The data of WHO classification, IDH mutation status and 1p/19q co-deletion were from the study of Ceccarelli, et al. [27] We then calculated the risk score using the regression coefficients of the identified prognostic signature of FDX1 for OS. Subsequently, we classified patients into the high-risk and low-risk groups according to the median value of risk scores.

Cox regression analysis was used to evaluate the relationship between FDX1 expression and survival indicators (overall survival, progress free interval and disease specific survival) of patients using the TCGA databases. The Kaplan–Meier method was used to assess the difference between "high" and "low" risk groups based on the best separation of FDX1 expression, employing R packages of "survminer" (version: 0.4.9) and "survival" (version: 3.2-10). Subsequently, the patients were divided into high and low FDX1 expression groups with the maximum-selected log-rank statistic. Log-rank *P* value, hazard ratio (HR), and 95%CI were examined. ROC curves were computed for presenting the prediction ability using the R package "survival ROC".

5.3 Establishment and evaluation of the nomogram

In the present study, FDX1 expression and the clinical stage were used to build a nomogram, which is an effective and convenient approach for estimating the overall survival in individual patients [28]. The calibration curve were performed to verify and estimate the prediction accuracy of the nomogram.

In addition, we investigated potential differences among subgroups stratified by IDH status, 1p/19q codeletion and primary therapy outcome. Enhanced regression nomograms of FDX1 and other clinical covariates of LGG patients were constructed by the R package "survival" (version 3.2-10) and "rms" (version 6.2-0). The prognosis types are Overall Survival. The calibration curves of the FDX1' scores and other clinical covariates of LGG patients were estimated. The data comes from RNA-seq data in level 3 HTSeq-FPKM format in the LGG Project of TCGA (https://portal.gdc.cancer.gov/), and $\log_2$ transformation is performed. Three data on WHO grade, IDH mutation status, and 1p/19q codeletion were obtained from the study of Ceccarelli, et al. [27]. Prognostic data were obtained from the work by Liu, et al. [26].

5.4 Expression of FDX1 protein and immune evaluation

The expression profiles of FDX1 in LGG were presented with TIMER (https://cistrome.shinyapps.io/timer/). TIMER database was used to evaluate the correlation between FDX1 expression and immune cell infiltration [29]. The TIMER database provided a crucial assessment and integration of immune cells for RNA sequencing samples from TCGA, including B cells, CD4+ T cells, CD8+ T cells, macrophages, neutrophils, and dendritic cells.

Correlation module draws the expression scatterplots between FDX1 and 3 key immune checkpoints (PDCD1, CD274, and HAVCR2), respectively, together with Spearman's rho value and estimated statistical significance, all available on the TIMER website.

5.5 Expression of FDX1 protein in LGG and meningioma

Immunohistochemical method was used to detect the expression of FDX1 in 5 LGG samples and 2 normal brain tissues. All the LGG patients received surgical treatment without preoperative chemoradiotherapy. The normal brain tissues were from meningioma patients. The immunohistochemistry images were scanning by the 3DHISTECH Pannoramic scan system, and quantitative analysis was processed using Image J software. This study was approved by the Ethical Committee of the Sixth Affiliated Hospital of Sun Yat-sen University (No. E2023092).

5.6 Statistical analysis

All statistical analyses were performed using R environment. P values were two-sided, and we considered a level of *P* value less than 0.05 to be statistically significant.

Conflict of interests

The authors declare no conflict of interests.

References

[1] Romera-Giner, S., Andreu Martínez, Z., García-García, F., Hilalgo, M. R. Common pathways and functional profiles reveal underlying patterns in Breast, Kidney and Lung cancers. *Biology Direct*, **2021**, 16: 9. https://doi.org/10.1186/s13062-021-00293-8

[2] Sung, H., Ferlay, J., Siegel, R. L., Laversanne, M., Soerjomataram, I., Jemal, A., Bray, F. Global Cancer Statistics 2020: GLOBOCAN Estimates of Incidence and Mortality Worldwide for 36 Cancers in 185 Countries. *CA: A Cancer Journal for Clinicians*, **2021**, 71(3): 209–249. https://doi.org/10.3322/caac.21660

[3] Minniti, G., Lombardi, G., Paolini, S. Glioblastoma in elderly patients: current management and future perspectives. *Cancers*, **2019**, 11(3): 336. https://doi.org/10.3390/cancers11030336

[4] Louis, D. N., Perry, A., Wesseling, P., Brat, D. J., Cree, I. A., Figarella-Branger, D., Hawkins, C., Ng, H. K., Pfister, S. M., Reifenberger, G., et al. The 2021 WHO Classification of Tumors of the Central Nervous System: A summary. *Neuro-Oncology*, **2021**, 23(8): 1231–1251. https://doi.org/10.1093/neuonc/noab106

[5] Qiu, X. W., Tian, Y. H., Xu, J. N., Jiang, X., Liu, Z. Y., Qi, X. W., Chang, X., Zhao, J. X., Huang, J. C. Development and validation of an immune-related long non-coding RNA Prognostic model in glioma. *Journal of Cancer*, **2021**, 12(14): 4264–4276. https://doi.org/10.7150/jca.53831

[6] Jin, H., Zhang, X. X., Su, J., Teng, Y. Q., Ren, H., Yang, L. Z. RNA interference-mediated knockdown of translationally controlled tumor protein induces apoptosis, and inhibits growth and invasion in glioma cells. *Molecular Medicine Reports*, **2015**, 12(5): 6617–6625. https://doi.org/10.3892/mmr.2015.4280

[7] Quail, D. F., Joyce, J. A. The microenvironmental landscape of brain tumors. *Cancer Cell*, **2017**, 31(3): 326–341. https://doi.org/10.1016/j.ccell.2017.02.009

[8] Cui, G., Wu, J., Lin, J., Liu, W., Chen, P., Yu, M., Zhou, D., Yao, G. *Journal of Nanobiotechnology*, **2021**, 19(1): 211. https://doi.org/10.1186/s12951-021-00902-8

[9] Hsu, H.-P., Wang, C.-Y., Hsieh, P.-Y., Fang, J.-H., Chen, Y.-L. Knockdown of serine/threonine-protein kinase 24 promotes tumorigenesis and myeloid-derived suppressor cell expansion in an

orthotopic immunocompetent gastric cancer animal model. *Journal of Cancer*, **2020**, 11(1): 213–228. https://doi.org/10.7150/jca.35821

[10] Tsvetkov, P., Coy, S., Petrova, B., Dreishpoon, M., Verma, A., Abdusamad, M., Rossen, J., Joesch-Cohen, L., Humeidi, R., Spangler, R. D., et al. Copper induces cell death by targeting lipoylated TCA cycle proteins. *Science*, **2022**, 375(6586): 1254–1261. https://doi.org/10.1126/science.abf0529

[11] Sheftel, A. D., Stehling, O., Pierik, A. J., Elsasser, H. P., Muhlenhoff, U., Webert, H., Hobler, A., Hannemann, F., Bernhardt, R., Lill, R. Humans possess two mitochondrial ferredoxins, Fdx1 and Fdx2, with distinct roles in steroidogenesis, heme, and Fe/S cluster biosynthesis. *Proceedings of the National Academy of Sciences*, **2010**, 107(26): 11775–11780. https://doi.org/10.1073/pnas.1004250107

[12] Ewen, K. M., Ringle, M., Bernhardt, R. Adrenodoxin—A versatile ferredoxin. *IUBMB Life*, **2012**, 64(6): 506–512. https://doi.org/10.1002/iub.1029

[13] Wang, M. J., Zhou, Z. J., Zheng, J. L., Xiao, W. X., Zhu, J. M., Zhang, C. C., Jiang, X. B. Identification and validation of a prognostic immune-related alternative splicing events signature for glioma. *Frontiers in Oncology*, **2021**, 11: 650153. https://doi.org/10.3389/fonc.2021.650153

[14] Xiao, C., Yang, L. H., Jin, L. Z., Lin, W. G., Zhang, F. Q., Huang, S. X., Huang, Z. J. Prognostic and immunological role of cuproptosis-related protein FDX1 in pan-cancer. *Frontiers in Genetics*, **2022**, 13: 962028. https://doi.org/10.3389/fgene.2022.962028

[15] Lu, H. W., Zhou, L. W., Zhang, B. C., Xie, Y. Y., Yang, H. Y., Wang, Z. X. Cuproptosis key gene FDX1 is a prognostic biomarker and associated with immune infiltration in glioma. *Frontiers in Medicine*, **2022**, 9: 939776. https://doi.org/10.3389/fmed.2022.939776

[16] Xu, J. H., Hu, Z. G., Cao, H., Zhang, H., Luo, P., Zhang, J., Wang, X. Y., Cheng, Q., Li, J. B. Multi-omics pan-cancer study of cuproptosis core gene *FDX1* and its role in kidney renal clear cell carcinoma. *Frontiers in Immunology*, **2022**, 13: 981764. https://doi.org/10.3389/fimmu.2022.981764

[17] Zhang, B. H., Xie, L., Ouyang, L. P., He, M. L. The expression and prognostic significance of FDX1 in glioma. *Lingnan Modern Clinics in Surgery*, **2022**, 22(05): 509–511.

[18] Zhu, H. X., Wan, Q. S., Tan, J. C., Ouyang, H. Y., Pan, X. Y., Li, M. H., Zhao, Y. Y. A novel prognostic signature of cuproptosis-related genes and the prognostic value of FDX1 in gliomas. *Frontiers in Genetics*, **2022**, 13: 992995. https://doi.org/10.3389/fgene.2022.992995

[19] Ye, Z., Zhang, S. Q., Cai, J. Y., Ye, L. G., Gao, L., Wang, Y. X., Tong, S. A., Sun, Q., Wu, Y., Xiong, X. X., Chen, Q. X. Development and validation of cuproptosis-associated prognostic signatures in WHO 2/3 glioma. *Frontiers in Oncology*, **2022**, 12: 967159. https://doi.org/10.3389/fonc.2022.967159

[20] Wang, J.-J., Wang, H., Zhu, B.-L., Wang, X., Qian, Y.-H., Xie, L., Wang, W.-J., Zhu, J., Chen, X.-Y., Wang, J.-M., Ding, Z.-L. Development of a prognostic model of glioma based on immune-related genes. *Oncology Letters*, **2021**, 21(2): 116. https://doi.org/10.3892/ol.2020.12377

[21] Bruni, D., Angell, H. K., Galon, J. The immune contexture and immunoscore in cancer prognosis and therapeutic efficacy. *Nature Reviews Cancer*, **2020**, 20(11): 662–680. https://doi.org/10.1038/s41568-020-0285-7

[22] Zhang, E. K., Ding, C. S., Li, S. C., Zhou, X. L., Aikemu, B., Fan, X. D., Sun, J., Zheng, M. H., Yang, X. Roles and mechanisms of tumour-infiltrating B cells in human cancer: a new force in immunotherapy. *Biomarker Research*, **2023**, 11(1): 28. https://doi.org/10.1186/s40364-023-00460-1

[23] Yang, X. D., Liu, X. S., Li, J. J., Zhang, P. P., Li, H. J., Chen, G. Q., Zhang, W., Wang, T. F., Frazer, I., Ni, G. Y. Caerin 1.1/1.9 enhances antitumour immunity by activating the IFN-α response signalling pathway of tumour macrophages. *Cancers*, **2022**, 14(23): 5785. https://doi.org/10.3390/cancers14235785

[24] Chen, Y. B., Song, Y. C., Du, W., Gong, L. L., Chang, H. C., Zou, Z. Z. Tumor-associated macrophages: an accomplice in solid tumor progression. *Journal of Biomedical Science*, **2019**, 26(1): 78. https://doi.org/10.1186/s12929-019-0568-z

[25] Vivian, J., Rao, A. A., Nothaft, F. A., Ketchum, C., Armstrong, J., Novak, A., Pfeil, J., Narkizian, J., Deran, A. D., Musselman-Brown, A., et al. Toil enables reproducible, open source, big biomedical data analyses. *Nature Biotechnology*, **2017**, 35(4): 314–316. https://doi.org/10.1038/nbt.3772

[26] Liu, J. F., Lichtenberg, T., Hoadley, K. A, Poissan, L. M., Lazar, A. J., Cherniack, A. D., Kovatich, A. J., Benz, C. C., Levine, D. A., Lee, A. V., et al. An integrated TCGA pan-cancer clinical data resource to drive high-quality survival outcome analytics. *Cell*, **2018**, 173(2): 400–416. https://doi.org/10.1016/j.cell.2018.02.052

[27] Ceccarelli, M., Barthel, F. P., Malta, T. M., Sabedot, T. S., Salama, S. R., Murray, B. A., Morozova, O., Newton, Y., Radenbaugh, A., Pagnotta, S. M., et al. Molecular profiling reveals biologically discrete subsets and pathways of progression in diffuse glioma. *Cell*, **2016**, 164(3): 550–563. https://doi.org/10.1016/j.cell.2015.12.028

[28] Park, S. Y. Nomogram: An analogue tool to deliver digital knowledge. *The Journal of Thoracic and Cardiovascular Surgery*, **2018**, 155(4): 1793. https://doi.org/10.1016/j.jtcvs.2017.12.107

[29] Li, B., Severson, E., Pignon, J. C., Zhao, H. Q., Li, T. W., Novak, J., Jiang, P., Shen, H., Aster, J. C., Rodig, S., et al. Comprehensive analyses of tumor immunity: Implications for cancer immunotherapy. *Genome Biology*, **2016**, 17(1): 174. https://doi.org/10.1186/s13059-016-1028-7